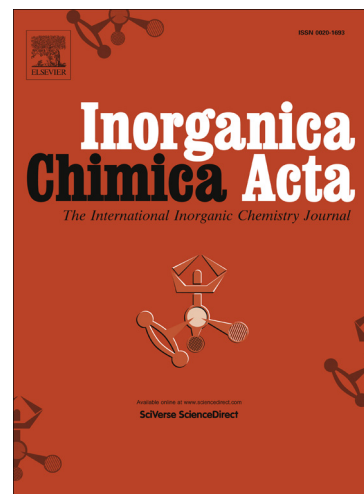# Accepted Manuscript

Near-infrared absorbing unsymmetrical Zn(II) phthalocyanine for dye-sensitized solar cells

Varun Kumar Singh, Paolo Salvatori, Anna Amat, Saurabh Agrawal, Filippo De Angelis, Md.K. Nazeeruddin, Narra Vamsi Krishna, Lingamallu Giribabu

Near-infrared absorbing unsymmetrical Zn(II) phthalocyanine for dye-sensitized solar cells

Varun Kumar Singh[a], Paolo Salvatori[b], Anna Amat[b], Saurabh Agrawal[b], Filippo De Angelis[b], Md. K. Nazeeruddin[c], Narra Vamsi Krishna[a], Lingamallu Giribabu[a]*

[a]*Inorganic & Physical Chemistry Division, CSIR-Indian Institute of Chemical Technology, Hyderabad 500607, India.*

[b]*Computational Laboratory for Hybrid/Organic Photovoltaics (CLHYO), Istituto CNR di Scienze Tecnologie Molecolari, Via Elce di Sotto 8, I-06123, Perugia, Italy.*

[c]*Laboratory for Photonics and Interfaces, Institute of Chemical Sciences and Engineering, School of basic Sciences, Swiss Federal Institute of Technology, CH - 1015 Lausanne, Switzerland.*

*Author for correspondence E-mail: giribabu@iict.res.in, **Phone:** +91-40-27193186, fax: +91-40-27160921

ABSTRACT: Unsymmetrical Zn phthalocyanine consisting of six S-aryl groups at -positions and a carboxy anchoring group at -position has been designed and synthesized for dye-sensitized solar cells (DSCs) applications. The unsymmetrical phthalocyanine has been characterized by elemental, MALDI-MS, IR, ^{1}H NMR, UV-Visible, fluorescence (steady-state & lifetime) and electrochemical (including spectroelectrochemical) methods. The Q-band absorption maxima of the unsymmetrical phthalocyanine was red-shifted due to the presence of S-aryl groups, which destabilizes the HOMO level consistent with electrochemical and *in-situ* spectroelectrochemical studies. The redox processes are assigned to the macrocyclic ring-based electron transfer processes, the LUMO of the unsymmetrical phthalocyanines lies above the TiO_2 conduction band, and the HOMO is well below the potential of the I^-/I_3^- redox electrolyte. The experimental results are supported by DFT/TD-DFT studies. The new unsymmetrical phthalocyanines was tested in DSCs using I^-/I_3^- redox electrolyte system.

KEYWORDS: Phthalocyanine, Unsymmetrycal phthalocyanine, Dye-sensitized solar cells, Spectroelectrochemal, Redox electrolyte.

1. INTRODUCTION

Dye-sensitized Solar Cells (DSCs) have become an actively pursued research topic both industrially and academically, which have the advantage of low embodied cost, easy to fabricate, and their performance is only moderately sensitive to temperature. [1-7]. Furthermore, DSCs can be fabricated on glass or flexible substrate, enabling a variety of aestetically appealing photovoltaic solutions. Typical DSCs consist of a photosensitizing dye, chemically grafted onto a wide bandgap semiconductor and a redox mediator which conducts the holes to a catalyst-coated (usually metallic platinum) cathode. The photosensitizing dye, which is a fundamental component of the device, harvests solar photons and initiates charge separation through photoinduced electron transfer from the dye excited state into the conduction band of TiO_2. The resulting oxidized dyes are subsequently reduced by the redox electrolyte. So far, among all the photosensitizers, ruthenium complexes have maintained a clear lead in DSC technology and in conjunction with the standard I^-/I_3^- redox mediator delivered a certified efficiency of 11.4% [8-14]. In spite of this, ruthenium complexes have limitations to mass commercialization owing to their rarity of the ruthenium metal and lack of absorption in the near infrared region.

In the search for ideal ruthenium-free metal sensitizers, 3d metal complexes Cu^{2+}, Ni^{2+}, Zn^2etc., and metal-free organic sensitizers have been designed for DSCs applications [15,16]. The highest reported DSCs efficiency exceeding 12% has been achieved by a Zn(II) porphyrin/organic dye cocktail [17]. Phthalocyanines, endowed with a large -conjugated framework, have also attracted considerable interest as solar cell sensitizers [18]. These dyes have also a remarkable thermal, chemical and photostability, which are highly required properties for long term working of DSCs. Despite having all these characteristics, phthalocyanines have shown poor to moderate performance as a consequence of their general tendency to form molecular aggregates and lack of solubility in common organic solvents. In the aggregated state, the electronic structure of the complexed Pc rings is perturbed resulting in an alteration of the ground state and excited state properties. Recently, several groups have designed and synthesized unsymmetrical phthalocyanines to improve the device efficiency [19-24]. But, in all these unsymmetrical phthalocyanine dyes, the Q-band absorption is narrow, which is centered around 700 nm, partly limiting the light-harvesting capability of the sensitized photoelectrodes.In order to further improve the efficiency of phthalocyanine based DSC devices, one has to shift the absorption maxima of the Q-band towards near-IR

region, along with a possible broadened absorption to enhance the spectral matching with the sunlight. In general, the Q-band absorption of phthalocyanine can be moved to longer wavelength through extension of -electron conjugation systems, such as moving towards naphthalocyanines and anthracyanines [25]. However, the LUMO levels of the later complexes seem to be lower than the phthalocyanine limiting their full exploitation in photovoltaic devices.

To cope with the above requirements, we have designed a new unsymmetrical phthalocyanine based on the '*push-pull*' concept, having S-aryl substituents at - positions of the macrocycle. The new phthalcyanine is having six bulky 4-*tert*-butyl benzenethiol groups (which act as electron releasing, '*push*') and one carboxyl acceptor (which act as electron withdrawing '*pull*' as well as anchoring group) in its molecular structure, see Scheme 1. The new unsymmetrical phthalocyanine has been characterized by elemental analysis, IR, MALDI-TOF, UV-Visible, fluorescence (steady-state & life-time) and electrochemical methods. A computational investigation was also performed to give a deeper insight on the optical and the electrochemical properties of this compound. Finally the new sensitizer has been tested in DSC devices, to assess its photovoltaic potential.

2. Experimental Section

2,3-dicyanohydroquinone, 3,4-dicyano benzoic acid, 4-*tert*-butyl benzethiol, DBU, and $Zn(OAc)_2.2H_2O$ were procured from Aldrich and used as such. Analytical reagent grade solvents were used for synthesis, and distilled laboratory grade solvents were used for chromatography. All solvents were procured from BDH (India) and were purified prior to use [26]. Milli-Q water was used for synthetic and purification purpose. ACME silica gel (100-200 mesh) was used for column chromatography and thin-layer chromatography was performed on Merck-precoated silica gel 60-F_{254} plates. Either gravity or flash chromatography was used for compound purification. Where a dual solvent system was used, gradient elution was employed, and the major band was collected.

2.1. Synthesis
Phthalonitrile-3,6-ditriflate (1): This compound was synthesized using the literature procedure [27]. 2,3-dicyanohydroquinone (4.80g, 30 mmol) was dissolved in dichloromethane (100 mL) and pyridine (5.93 g, 75 mmol). To this, triflic anhydride (21.16

g, 75 mmol) was added under nitrogen atmosphere at -78^0C. The reaction mixture was allowed to warm to room temperature and the stirring was continued for 24 h. The mixture was poured into water and the organic layer was extracted with dichloromethane. The extract was washed subsequently with water, 2% hydrochloric acid, water, brine and dried on sodium sulphate and filtered. The filtrate was evaporated on rotary evaporator. The crude product was then recrystallized from dichloromethane to obtain the desired compound. Elemental analysis of $C_{10}H_2F_6N_2O_6S_2$ (calculated mass % in parentheses): C, 28.35 (28.31); H, 0.50 (0.48); N, 6.61 (6.60). ^{1}H NMR (500 MHz, CDCl$_3$):   7.99 (s, 2H); FT IR(KBr): cm^{-1} 3114 ($_{C-H}$), 2254 ($_{C-N}$), 1602 ($_{C-C}$), 1474 ($_{C-C}$), 1440 ($_{C-C}$), 1133 ($_{S=O}$).

3,6-bis(thiophenyl-*tert*-butyl)phthalonitrile (2): *tert*-butylthiophenol (0.784 g, 4.72 mmol), was added to a stirred mixture of **1 (**1.0 g, 2.36 mmol), potassium carbonate (0.96 g) in dimethylsulfoxide (15 mL) solvent under the nitrogen atmosphere. The stirring was continued at room temperature for 24 h. After the reaction mixture was poured into water and the organic layer was extracted with dichloromethane, dried on sodium sulphate, then filtered. The filtrate was evaporated on rotary evaporator. The crude product was then washed with methanol and recrystallized from toluene to obtain the desired compound as yellow solid. Elemental analysis of $C_{28}H_{28}N_2S_2$ (calculated mass % in parentheses): C, 73.60 (73.64); H, 6.20 (6.18); N, 6.10 (6.13). ^{1}H NMR **(**300 MHz, DMSO-d^6):   7.46-7.39 (m, 8H), 7.00 (s, 2H), 1.31 (s, 12H); FT IR(KBr): cm^{-1} 3058 ($_{C-H}$), 2958 ($_{C-H}$), 2215 ($_{C-N}$), 1667 ($_{C-C}$), 1530 ($_{C-C}$), 1482 ($_{C-C}$), 1262, 830 (C-H).

Zn-Thio-Pc: A 50 ml round bottom flask was charged with **2** (1.0 g, 2.19 mmol), 3,4-dicyano benzoic acid (0.126 g, 0.73 mmol), Zn(OAc)$_2$ (0.208 g, 0.949 mmol) and dry 1-Pentanol (5 mL) and heated at 100^0C. To this catalyst, 1,8-diazabicyclo[5.4.0]undec-7-ene (DBU) was added and the resultant solution was heated to 140^0 C for 20 h and then cooled to room temperature. Pentanol was then removed under high vacuum and the solid green material was precipitated from methanol which was then subjected to silica gel column chromatography and eluted with hexane-chloroform to chloroform-methanol. The green phthalocyanine compound (second fraction) obtained was reprecipitated from methanol to afford the pure compound. Elemental analysis of $C_{93}H_{88}N_8O_2S_6Zn$ (calculated mass % in parentheses): C, 69.50 (69.49); H, 5.55 (5.52); N, 7.00 (6.97). MALDI-TOF:

($C_{93}H_{88}N_8O_2S_6Zn$)m/z: 1604 (M^+), 1605 ; FT IR(KBr): cm^{-1} 3444 ($_{O-H}$), 1687 ($_{C=O}$); UV-Vis ($_{max}$, nm) in THF: 750 (4.84), 676 (4.29), 350 (4.59).

2.2. Methods

The UV-Visible spectra were recorded with a Shimadzu model-170 spectrophotometer using 1×10^{-6} M solutions in THF solvent. Steady state fluorescence spectra were recorded using a Spex model Fluorlog-3 spectrofluorometer for solutions having optical density at the wavelength of excitation ($_{ex}$) 0.11. Time-resolved fluorescence measurements have been carried out using HORIBA Jobin Yvon spectrofluorometer. Briefly, the samples were excited at 670 nm and the emission was monitored at 780 nm. The count rates employed were typically $10^3 - 10^4\ s^{-1}$. Deconvolution of the data was carried out by the method of iterative reconvolution of the instrument response function and the assumed decay function using DAS-6 software.The goodness of the fit of the experimental data to the assumed decay function was judged by the standard statistical tests (*i.e.*, random distribution of weighted residuals, the autocorrelation function and the values of reduced ^{2}).MALDI-MS spectra were recorded on a TO-4X KOMPACT SEQ, KARTOS, UK, mass spectrometer. Major fragmentations are given as percentages relative to the base peak intensity. ^{1}H NMR spectra were obtained at 300 MHz using a Brucker 300 Avance NMR spectrometer running X-WIN NMR software. The elemental analyses were done on an Elementar, Vario MICRO CUBE analyzer.

Cyclic voltammetric measurements were performed on a PC-controlled CH instruments model CHI 620C electrochemical analyzer using 1 mM unsymmetrical phthalocyanine solution in THF solvent at scan rate of 100 mV/s with 0.1 M tetrabutyl ammonium perchlorate (TBAP) as supporting electrolyte. The working electrode is glassy carbon, standard calomel electrode (SCE) is reference electrode and platinum wire is an auxiliary electrode. After a cyclic voltammogram (CV) had been recorded, ferrocene was added, and a second voltammogram was measured.

2.2.1 Dye cell preparation

The TiO$_2$ photoelectrode fabrication is similarto our earlier studies [12,20].FTO glass (TEC-15, 2.2 mm thickness, Solaronix) was used for transparent conducting electrodes. The substrate was first cleaned in an ultrasonic bath using a detergent solution, acetone and

ethanol respectively (each step 15 min. long). The FTO glass plates were immersed into a 40mM aqueous $TiCl_4$ solution at 70 °C for 30 min and washed with water and ethanol. A layer of opaque TiO_2 paste (18NR-AO, Dyesol) was spread on the FTO glass plates by doctor blade. The TiO_2 layer was treated in an ethanol chamber and dried for 5min at 120°C. The TiO_2 coated electrodes (active area 0.2 cm^2) were gradually heated under air flow at 325 °C for 5 min, at 375 °C for 5 min, at 450 °C for 15 min, and 500 °C for 15 min. After the sintering process, the TiO_2 film was treated with 40mM $TiCl_4$ solution, then rinsed with water and ethanol. The electrodes were heated at 500 °C for 30 min and after cooling (80 °C) were immersed for 18 hours into sensitizing baths. These consisted of the Zn-Thio-Pc dye in 0.2 mM concentration in Ethanol:THF=9:1, and when required with 5 and 20.0 mM of 3a,7a-dihydroxy-5b-cholic acid (CDCA) added.

Counter electrodes were prepared by coating with a drop of H_2PtCl_6 solution (2 mg of Pt in 1 mL of ethanol) a FTO plate (TEC 15/2.2 mm thickness, Solaronix) and heating at 400 °C for 15 min. The TiO_2 sensitized photoanode and Pt counter electrode were assembled into a sealed sandwich-type cell by a hot-melt ionomer film (Surlyn, 25 μm thickness, Dyesol). The electrolyte solution was inserted by vacuum backfilling. Then, the hole was sealed by using additional Surlyn patch and a cover glass and finally a conductive Ag-based paint was deposed at the electrical contacts.

The Iolitech ES-0004 HP electrolyte, containing 1-butyl-3methylimidiazolium iodide, iodine, guanidinium thiocyanate and *tert*-butylpyridine, in a mixture of valeronitrile and acetonitrile, with LiI in 0.1M concentration added was used.

2.2.2. Photovoltaic Characterization

Photovoltaic measurements were recorded by means of AM 1.5 solar simulator equipped with a Xenon lamp (LOT-ORIEL LS 0106). The power of incoming radiation, set at 100 mW/cm^2, was checked by a piranometer. J–V curves were obtained by applying an external bias to the cell and measuring the generated photocurrent with a Keithley model 2400 digital source-meter, under the control of dedicated LabTracer 2.0 software. A black shading mask was employed to avoid the overestimation of the measured parameters.

2.2.3. Computational Details

DFT and TD-DFT calculations were performed using Becke's hybrid exchange functional B3 [28] with the Lee–Yang–Parr correlation functional LYP [29, 30] (B3LYP) and 6-31G** basis set [31]. Solvent effects for TetraHydroFuran (THF) were added using polarizable continuum model of solvation (PCM) [32, 33]as implemented in the Gaussian 09 software suit [34]. The absorption spectra have been simulated in THF solution by computing the first 40 singlet-singlet excitations; the computed spectra have been analysed in terms of the molecular orbital composition of the main transitions. Further, to gain insight on the interactions between the dye and the semiconductor, the adsorption of the dye onto a TiO_2model has been also investigated using a neutral cluster of 82 units of TiO_2 units (about 2x2 nm) exposing the anatase 101 surface; this model has demonstrated to give good results in previous studies [35].For computational convenience, a reduced dye model with hydrogen atoms replacing the tert-butyl substituents of the real system, Zn-Thio-Pc-M,was employed to simulate dye adsorption on to TiO_2.A single point calculation including the solvent effects at the same level of theory of that used for the isolated dyes has been performed in the dye@$(TiO_2)_{82}$ cluster. The density of states (DOS) for the first 100 unoccupied states has been described using a gaussian convolution with a σ of 0.2 for the whole joint system as well as the projection of the electronic states of the dye and of the semiconductor states.

3. Results and Discussion

The synthetic scheme of Zn-Thio-Pc is shown in Scheme 1. The Phthalonitrile-3,6-ditriflate (**1**) was synthesized by the condensation of 2,3-dicyanohydroquinone with triflic anhydride. Whereas 3,6-bis(thiophenyl-*tert*-butyl)phthalonitrile (**2**) was synthesized by condensation of **1** with *tert*-butylthiophenol. In both cases, pure phthalonitriles were obtained after recrystallization. Finally, the unsymmetrical phthalocyanine was obtained by cross-condensation of 2 with 3,4-dicyano benzoic acid using $Zn(OAc)_2$ as template and DBU as catalyst to get different isomers. The desired isomer was isolated by adopting silica gel column chromatography. The new unsymmetrical phthalocyanine is characterized by elemental analysis, Mass, IR, ^{1}H NMR, and fluorescence spectroscopies (both steady-state and time-resolved) as well as cyclic voltammetry (including spectroelectrochemistry). MALDI-MS spectrum consists of a molecular ion peak at 1605 that is assigned to the presence of corresponding unsymmetrical phthalocyanine.

3.1. Optical properties

The electronic absorption spectrum of Zn-Thio-Pc was recorded in THF solution and compared to that of the phthalocyanine adsorbed onto 2 m thick nanocrystalline TiO_2 films (see Figure 1).The absorption spectrum in solution consists of a low intensity Soret band at 350 nm (= 39,910 $M^{-1}cm^{-1}$) and a much more intense Q-band at 750 nm (= 69,300 $M^{-1}cm^{-1}$). The significant intensity of these bands compared to the ruthenium dyesis the result of the - * transitions in the macrocyclic system. The absorption maxima of Q-band are shifted towards the red region due to the presence of six S-aryl groups at -positions of the phthalocyanine macrocycle compared to the unsubstituted phthalocyanine. A similar bathochromic effect was observed in other S-aryl symmetrical phthalocyanines [36-38].

A comparative plot of the experimental and calculated UV-vis optical absorption spectra for the real Zn-Thio-Pc and for the reduced Zn-Thio-Pc-M model (see Computational details) systems along with their optimized geometries are given in Figure 2 and in Supporting Information.The calculated spectra for both molecules are in good agreement with the experimentally observed Soret band at 350 nm (3.54 eV) as well as Q-band at 750 nm (1.65 eV) (Table 1). Calculated UV-Visible spectrum for Zn-Thio-Pc molecule gives Soret band at 355 nm (3.49 eV) and Q-band at 744 nm (1.67 eV). Similarly, calculated absorption spectrum for Zn-Thio-Pc-M molecule shows Soret band at 346 nm (3.58 eV) and Q-band at 742 nm (1.67 eV).

Our calculations on both + systems show that the lowest two transitions constitute the Q-band. The first transition (S1) shows charge transfer from HOMO to LUMO. For both systems, the HOMO shows π character and is delocalized on the phthalocyanine ring. Whereas,the LUMO shows π^* character and is delocalized over phthalocyanine ring as well as carboxylic acid anchor (Figure 4). The charge distribution of these MOs involved in the S1 transition suggests a charge push from phthalocyanine ring towards the anchor moiety. The second transition (S2) also possesses highest oscillator strength (f) and shows HOMO→LUMO+1 character. Similar to the LUMO, the LUMO+1 is also delocalized on phthalocyanine ring but shows no localization on the carboxylic acid anchor (Figure 3). Several low intensity excitations contribute in formation of Soret band, see Table for a survey of the most relevant ones.

The absorption spectrum of the phthalocyanine adsorbed onto 2 m thick TiO_2 electrode is similar to that of the solution spectra but exhibits a small red shift (Fig. 1), which is due to Ti^{4+} acts as electron withdrawing and produces a red shift in the absorption bands. Figure 1 also shows the emission spectrum of Zn-Thio-Pc was obtained at room temperature

in THF solvent. The emission maximum was observed at 800 nm. The excitation spectrum obtained by exciting emission maximum at 800 nm shows a maximum at 750 nm and E_{0-0} energy of Zn-Thio-Pc estimated from excitation and emission spectra is 1.66 eV. Quenched emission spectrum was observed when the Zn-Thio-Pc adsorbed onto 2 m thick TiO_2 layer as a consequence of electron injection from the excited state of phthalocyanine into conduction of band of TiO_2. The singlet excited life-time of Zn-Thio-Pc was measured in THF solvent and found 2 ns (*See* Supporting information). Quenched life-time of <200 ps was observed when the unsymmetrical phthalocyanine anchored on to nanocrystalline TiO_2.

3.2. Electrochemical properties

With a view to evaluate the HOMO-LUMO levels of Zn-Thio-Pc, we have performed the electrochemistry by using cyclic voltammetric technique in THF solvent. The cyclic voltammogram of Zn-Thio-Pc is shown in Figure 4.Zn-Thio-Pc exhibits a quasireversible one-electron oxidations at 0.72 V, generating -cation radical and either reversible or quasireversible reductions were observed at –0.98 & -1.40 V. With respect to dye-sensitization of wide-bandgap semiconductors, e.g. TiO_2, the first oxidation potentials of Zn-Thio-Pc and the E_{0-0} transition energy, the energy levels of the singlet excited states (LUMO) of Zn-Thio-Pc was determined to be -0.94 V vs. SCE, whereas the energy level of the conduction band edge of TiO_2 is ca. –0.74 V vs. SCE [40]. This makes electron injection from the excited state of Zn-Thio-Pc into the conduction band of TiO_2 thermodynamically feasible. Furthermore, the HOMO level of the Zn-Thio-Pc is lower than the energy level of the redox couple I^-/I_3^- (0.2 V vs. SCE) in the electrolyte, enabling the dye regeneration by electron transfer from I^-.

Spectroelectrochemical studies were employed to confirm the assignments of the electron transfer reactions recorded with CV measurements of Zn-Thio-Pc. This information is essential concerning the durability of the sensitizer. Figure 5 represents *in-situ* UV-vis spectral changes in THF/TBAP under applied potential.

During the first oxidation process (E_{app} = 0.90V), the absorption Q-band decreases in intensity without shift, while new band is appeared at 900 nm with increase in intensity, whereas the intensity of Soret band increases. The band assigned to the aggregated species at 680 nm is also decreases in intensity due to the shifting of the aggregation-disaggregation equilibrium under applied potential. The process gives clear well-defined isosbestic point at 360, 600 and 790 nm, which indicate the formation of one type of oxidizedspecies. These

spectroscopic changes (Fig. 6a) indicate presences of an aggregation-disaggregation equilibrium and a macrocycle ring oxidation process and the oxidation process assigned to $[Zn^{II}Pc^{-2}]/[Zn^{II}Pc^{-1}]^{+1}$ process [41-43]. The unsymmetrical phthalocyanine return to original absorption spectrum, if once applied potential removed. During the reduction of Zn-Thio-Pc (applied potential at -1.2 V), the absorption of Q-band intensity decreases whereas the intensity of Soret increases without shift. During this process clear isosbestic points are observed at 390, 400, and 620 nm, which clearly indicates that the reduction gives a single product. These changes are typical of the ring-based reduction and assigned to $[Zn^{II}Pc^{-2}]/[Zn^{II}Pc^{-3}]^{-1}$. As shown in Figure 3c, under the applied potential at -1.70 V, the intensity of Q-band absorption further decreases and Soret band intensity increases with appearance of new bands at 580 and 900 nm with increasing intensity. The aggregation band at 680 nm completely disappeared. This process gives clear isosbestic points at 380, 400, 640 and 790 nm. Spectroscopic changes under controlled potential application at -1.70 V supported the further reduction of the monoanionic $[Zn^{II}Pc^{-3}]^{-1}$ species to $[Zn^{II}Pc^{-4}]^{-2}$.

3.3. DFT/TD-DFT calculations

In order to have a deeper understanding of the charge-transfer ability of Zn-Thio-Pc-M molecule upon chemisorption on TiO_2, and to gain insight into the dye adsorption mode on to the semiconductor surface, we have investigated the electronic structure of Zn-Thio-Pc-M@TiO_2 complex using Density of States (DOS) plot for unoccupied orbitals (Figure 6).

The unoccupied DOS profile shows that upon interaction with TiO_2, the dye LUMO is substantially broadened, reflecting a good propension for the dye to inject charge into the TiO_2conduction band. Inspection of the optimized dye adsorption geometry onto TiO_2 (Fig. 7) reveals a possible hindrance of the tio-aryl substituents with the TiO_2 surface, which might lead to sensitization problems, see below. On further analysis of individual unoccupied orbitals, we found that the LUMO of Zn-Thio-Pc-M reallocates to LUMO+30 of Zn-Thio-Pc-M@TiO_2 and the LUMO+1 is found as the LUMO+31 of Zn-Thio-Pc-M@TiO_2. The isosurface plot for LUMO+1 of Zn-Thio-Pc-M (Figure 3) and LUMO+31 of Zn-Thio-Pc-M@TiO_2 (Figure 7) shows that both MOs are characteristically similar. Furthermore, comparative MO alignment plot (Figure 8) shows that the dye-based unoccupied orbitals of Zn-Thio-Pc-M@TiO_2 are well aligned with the TiO_2 conduction band, lying at least ca. 0.5 eV above the conduction band edge.

3.4. Photovoltaic Studies

Photovoltaic tests have been finally conducted using the new sensitizer. The measured parameters and the *JV*-curves are reported respectively in Table 3 and Figure 9.

Since the absorption spectra have shown a slight red shift and a moderate broadening of the Q-band moving from the solution to the TiO_2, suggesting weak aggregation issues, the first test was made without using the Chenodeoxycholic Acid (CDCA) coadsorbent in the dye solution (Cell 1). A conversion efficiency of 0.4% was reached, due to the combination of poor J_{sc} (1.26 mA/cm2) and V_{oc} (0.5 V). These disappointing values of J_{sc} and V_{oc} could be explained with the poor electron injection from the excited state of the macrocycle into the semiconductor conduction band and to the fast recombination process of the injected electrons with the oxidized dye. Another important issue affecting the electron injection, anyway, might be the dye aggregation. To overcome this problem the use of CDCA disaggregant in 0.02M concentration was tested (Cell 2). Unfortunately, in these conditions, the CDCA is highly competitive with the Zn-Thio-Pc dye for the TiO_2 binding sites, leading to a poor photoanode sensitization. This translates into a a strong photocurrent reduction upon increasing the CDCA content,which further diminishes the photovoltaic performances to 0.22 and 0.14% efficiency.

Finally, we have examined the thermal stability of Zn-Thio-Pcby using thermogravimetric analysis for outdoor applications. Figure 10 shows the thermal behavior of Zn-Thio-Pc. It is known from the literature that phthalocyanine and its metallo derivatives are stable up to 400 ^{o}C [44]. The thermograme indicates that the Zn-Thio-Pc sensitizer is stable up to 250 ^{o}C. The weight loss (up to 3.42 %) was observed in 250 - 350 ^{o}C temperature is attributed to the removal of the carboxyl group from the macrocycle.

4. Conclusions

In conclusion, we have synthesized an unsymmetrical S-aryl zinc phthalocyanine based on '*push-pull*' concept having six S-aryl groups at non-peripheral positions of phthalocyanine macrycycl, which act as electron releasing (*push*). It also has a carboxyl group acts as electron withdrawing groups (*pull*) and server to graft on to nanocrystalline TiO_2. Photophysical properties (absorption, emission and redox properties) indicate that the LUMO of unsymmetrical phthalocyanines is quite above the TiO_2 conduction band, as also computationally verified, and the HOMO is sufficiently below the potential of the I^-/I_3^- redox electrolyte.Spectroelectrochemical studies indicate that the electron transfer processes are ring-centered and not metal-centered processes. The new unsymmetrical phthalocyanine was

tested in DSSC using I^-/I_3^- redox couple and offered low overall conversion efficiencies. The reason for the rather modest efficiency values is probably due to the weak sensitization of the TiO_2 semiconductor, rather than to dye aggregation, as demonstrated by the detrimental effect of the CDCA coa-adosorbent. Computational anaylses suggest indeed that the bulky tert-butyl substituents, although preventing dye aggregation, also contribute some hindrance to the dye interaction with the semiconductor surface.

Acknowledgements

References:

1. B. O'Regan, M. Grätzel M, *Nature* 353 (1991) 737-740.

2. M. Grätzel, *Nature* 414 (2001) 338-344.

3. N. Robertson, *Angew. Chem. Int. Ed*. 45 (2006) 2338-2345.

4. M. Grätzel, *Acc. Chem. Res*. 42 (2009) 1788-1798.

5. J.W. Bowers, H.M. Upadhyaya, S. Calnan, R. Hashimoto, T. Nakada, A.N. Tiwari, *Prog. Photovoltaics: Research & Applications*, 17 (2009) 265-272.

6. A. Hagfeldt, G. Boschloo, L. Sun, L. Kloo, H. Pettersson, *Chem. Rev.* 110 (2010) 6595–6663.

7. L. Giribabu, K. Sudhakar, K. Velkannan, *Current Sci*. 102 (2012) 991-1000.

8. M.K. Nazeeruddin, P. Pechy, T. Renouard, S.M. Zakeeruddin, R. Humphry-Baker, P. Comte, P. Liska, L. Cevey, E. Costa, V. Shklover, L. Spiccia, G.B. Deacon, C.A. Bignozzi, M. Grätzel, *J. Am. Chem. Soc*., 123 (2001) 1613-1624.

9. P. Wang, S.M. Zakeeruddin, J.E. Moser, M.K. Nazeeruddin, T. Sekiguchi, M. Grätzel, *Nat. Mater*. 2 (2003) 402-407.

10. L. Giribabu, Ch.V. Kumar, Ch.S. Rao, V.G. Reddy, P.Y. Reddy, M. Chandrasekharam, Y. Soujanya, *Energy Environ. Sci*. 2 (2009) 770-773.

11. T. Bessho, E. Yoneda, J-H. Yum, M. Guglielmi, I. Tavernelli, H. Imai, U. Rothlisberger, M.K. Nazeeruddin, M. Grätzel, *J. Am. Chem. Soc*. 131 (2009) 5930-5934.

12. L. Giribabu, T. Bessho, M. Srinivasu, C. Vijaykumar, Y. Soujanya, V.G. Reddy, P.Y. Reddy, J.H. Yum, M. Grätzel, M.K. Nazeeruddin, *Dalton Trans*. 40 (2011) 4497-504.

13. A. Abbotto, F. Sauvage, C. Barolo, F. De Angelis, S. Fantacci, M. Grätzel, N. Manfredi, C. Marinzi M.K. Nazeeruddin, *Dalton Trans* 40 (2011) 234-242.

14. L. Han, A. Islam, H. Chen, C. Malapaka, B. Chiranjeevi, S. Zhang, X. Yang M. Yanagida, *Energy Environ. Sci*. 5 (2012) 6057-6060.

15. L. Giribabu, R.K. Kanaparthi, V.Velkannan *The Chemical Record* 12 (2012) 306-328.

16. R.K. Kanaparthi, J. Kandhadi,L. Giribabu *Tetrahedron* 68 (2012) 8383-8393.

17. A. Yella, H-W. Lee, H.N. Tsao, Yi C, A.K. Chandiran, M.K. Nazeeruddin, E.W-G. Diau, C-Y. Yeh, S.M. Zakeeruddin, M. Grätzel, *Science* 334 (2011) 629-634.

18. A.L.Thomas,Ed.''PhthalocyanineResearchandApplications,CRC Press, Boston, 1990.

19. P.Y. Reddy, L. Giribabu, Ch. Lyness, H.J. Snaith, Ch. Vijaykumar, M. Chandrasekharam, M.L. Kantam, J-H. Yum, K. Kalyanasundaram, M. Grätzel M.K.Nazeeruddin, *Angew. Chem. Int. Ed. Engl*. 46 (2007) 373–376.

20. L. Giribabu, Ch. Vijaykumar, V.G. Reddy, P.Y. Reddy, Ch.S. Rao, S-R. Jang, J-H. Yum, M.K. Nazeeruddin, M.Grätzel *Solar Energy Materials & Solar Cells*. 91 (2007) 1611-1617.

21. J.J. Cid, M. Gracia-Iglesias, J-H. Yum, A. Forneli, J. Albero, P. Vazquez, M. Grätzel, M.K. Nazeeruddin, E. Palomares, T. Torres, *Chem. Eur. J*. 15 (2009) 5130-5137.

22. S. Mori, M. Nagata, Y. Nakahata, K. Yasuta, R. Goto, M. Kimura, M. Taya. *J. Am. Chem. Soc*. 132 (2010) 4054-4055.

23. L. Giribabu, V.K. Singh, Ch.V. Kumar, Y. Soujanya, P.Y. Reddy, M.L. Kantam. *Solar Energy* 85 (2011) 1204-1212.

24. M-E. Ragoussi, J-J. Cid, J-H. Yum, G. delaTorre, D.D. Censo, M. Grätzel, M.K. Nazeeruddin, T.Torres Angew. Chem. Int. Ed. Engl. 51 (2012) 4375-4378.

25. E Ohono, K. Sakamot, N.K. Kaishi, J. Chem., Soc. Jan, Chem. Ind. Chem. (1995) 730–735.

26. "Purification of Laboratory Chemicals," Ed.'s W.L.F. Armango, Ch.L.L. Chai 2003, Butterworth Heinemann, NewYork.

27. K. Sakamoto, E. Ohno-Okumura, T. Kato, H. Soga *J. Porphyrins & Phthalocyanines* 14 (2010) 47-54.

28. A.D. Becke *J. Chem. Phys.*; 98 (1993) 5648–5652.

29. C. Lee, W. Yang, R.G. Parr, *Phys. Rev. B*.; 37 (1998) 785–789.

30. B. Miehlich, A. Savin, H. Stoll, H. Preuss,*Chem. Phys. Lett.*; 157 (1989) 200–206.

31. G.A. Petersson, M.A. Al-Laham, *J. Chem. Phys.*; 94 (1991) 6081-6090.

32. M. Cossi, N. Rega, G. Scalmani, V.J. Barone. *Comp. Chem*. 24 (2003) 669-681.

33. M. Pastore, F. De Angelis, *Phys. Chem. Chem. Phys*. 14 (2012) 920-928.

34. Gaussian 09, A.L. Revision, M.J. Frisch, G.W. Trucks, H.B. Schlegel, G.E. Scuseria, M.A. Robb, J.R. Cheeseman, G. Scalmani, V. Barone, B. Mennucci, G.A. Petersson, H. Nakatsuji, M. Caricato, X. Li, H.P. Hratchian, A.F. Izmaylov, J. Bloino, G. Zheng, J.L. Sonnenberg, M. Hada, M. Ehara, K. Toyota, R. Fukuda, J. Hasegawa, M. Ishida, T. Nakajima, Y. Honda, O. Kitao, H. Nakai, T. Vreven, J.A. Montgomery Jr., J.E. Peralta, F. Ogliaro, M. Bearpark, J.J. Heyd, E. Brothers, K.N. Kudin, V.N. Staroverov, R. Kobayashi, J. Normand, K. Raghavachari, A. Rendell, J.C. Burant, S.S. Iyengar, J. Tomasi, M. Cossi, N. Rega, J.M. Millam, M. Klene, J.E. Knox, J.B. Cross, V. Bakken, C. Adamo, J. Jaramillo, R. Gomperts, R.E. Stratmann, O. Yazyev, A.J. Austin, R. Cammi, C. Pomelli, J.W. Ochterski, R.L. Martin, K. Morokuma, V.G. Zakrzewski, G.A. Voth, P. Salvador, J.J. Dannenberg, S. Dapprich, A.D. Daniels, Ö. Farkas, J.B. Foresman, J.V. Ortiz, J. Cioslowski, D.J. Fox, Gaussian, Inc., Wallingford CT, 2009.

35. F. De Angelis, S. Fantacci, E. Mosconi, M.K. Nazeeruddin, M. Grätzel, *J. Phys. Chem. C,* 115 (2011) 8825-8831.

36. P.M. Burnham, M.J. Cook, L.A. Gerrard, M.J. Heeney, D.L. Hughes *Chem. Commun*. (2003) 2064–2065.

37. M.J. Cook, A.J. Dunn, A.J. Thomson, K.J. Harrison. *J. Chem. Soc., Perkin Trans*. I (1998) 2453–2458.

38. T. Ouguchi, S. Aihara JP 1992–04015265, Chem. Abstr. 117 (1992) 61660.

39. M.K. Nazeeruddin, R. Splivallo, P. Liska, P. Comte, M. Grätzel *Chem. Commun*., (2003) 1456-1457.

40. A. Hagfeldt, M. Grätzel *Chem. Rev*. 95 (1995) 49-68.

41. B. Simicglavaski, S. Zecevic, E. Yeager, *J Electrochem Soc* 134 (1987) C130.

42. B. Agboola, K.I. Ozoemena, T. Nyokong. *Electrochim Acta* 51 (2006) 4379-4387.

43. Z. Ou, Z. Jiang, N. Chen, J. Huang, J. Shen, K.M..Kadish *J. Porphyrins & Phthalocyanines* 12 (2008) 1123-33.

44. X. Wei, X. Du, D. Chen, Z. Chen, *Thermochimica Acta*, 440 (2006) 181-187 (and references therein).

Captions:

Scheme 1: Synthetic scheme of **Zn-Thio-Pc**.

Fig. 1: UV-Visible spectra of Zn-Thio-Pc (———) THF, (------) adsorbed onto a 2 m thick TiO$_2$ film,(———) emission spectra in THF solvent.

Fig. 2: Experimental (black) and calculated (blue) (FWHM = 0.37 eV) UV-visible spectra of Zn-Thio-Pc dye. Blue vertical lines correspond to calculated excitation energies and oscillator strength.

Fig. 3: Electron density plots of H-1, H, L and L+1 of Zn-Thio-Pc (top) and Zn-Thio-Pc-M (bottom).

Fig. 4: Cyclic voltammogram of **Zn-Thio-Pc** in THF solvent.

Fig 5: *In-Situ* UV-Vis spectral changes of **Zn-Thio-Pc** a) E$_{app}$ = 0.90 V. b) initial part of the spectral changes at E$_{app}$ = -1.20 V, c) final part of the spectral changes at E$_{app}$ = -1.80 V.

Fig. 6: Density of states (DOS) plot (using 101 lowest unoccupied states) for (a) Zn-Thio-Pc-M moiety (green), (b) TiO$_2$ (blue) and (c) Zn-Thio-Pc-M@TiO$_2$ (red).

Fig. 7: Electron density plot of L+31 of Zn-Thio-Pc-M@TiO$_2$ complex

Fig. 8: Comparative alignment MOs of (A) Zn-Thio-Pc, (B) Zn-Thio-Pc-M and (C) Zn-Thio-Pc-M@TiO$_2$ systems. Values given in the plot correspond to the HOMO and LUMO gap in eV.

Fig. 9: *J-V* characteristics of cells of Table 3. Cell 1, without CDCA (blue line); cell 2, with CDCA 0.02M (red line) and cell 3 with CDCA 0.005M (green line).

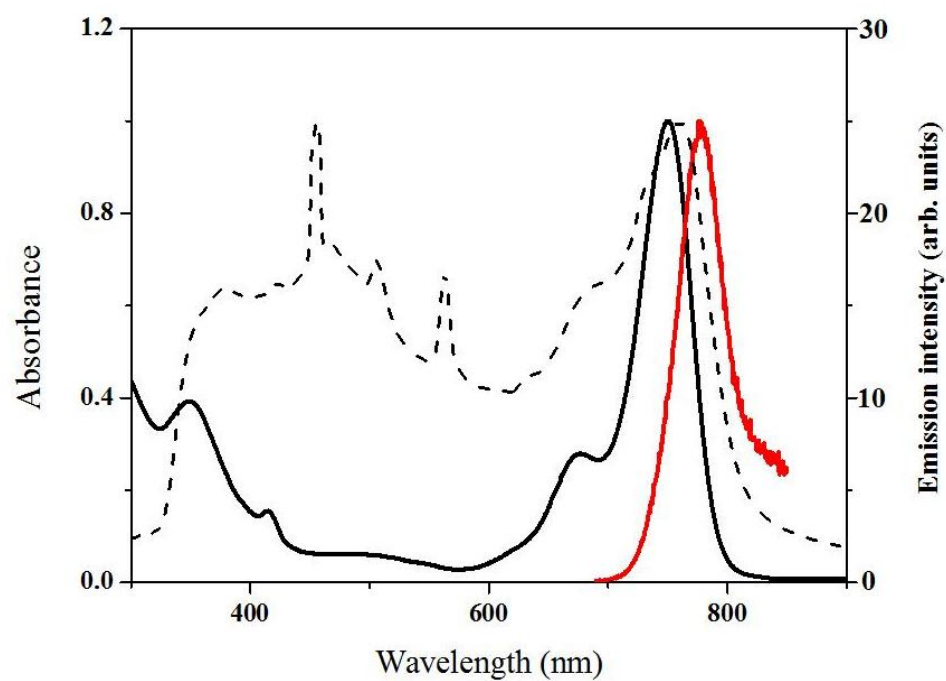**Fig. 10:** TG/DTG curves of **Zn-Thio-Pc** with heating rate of 10 ^{o}C min-1 under nitrogen.
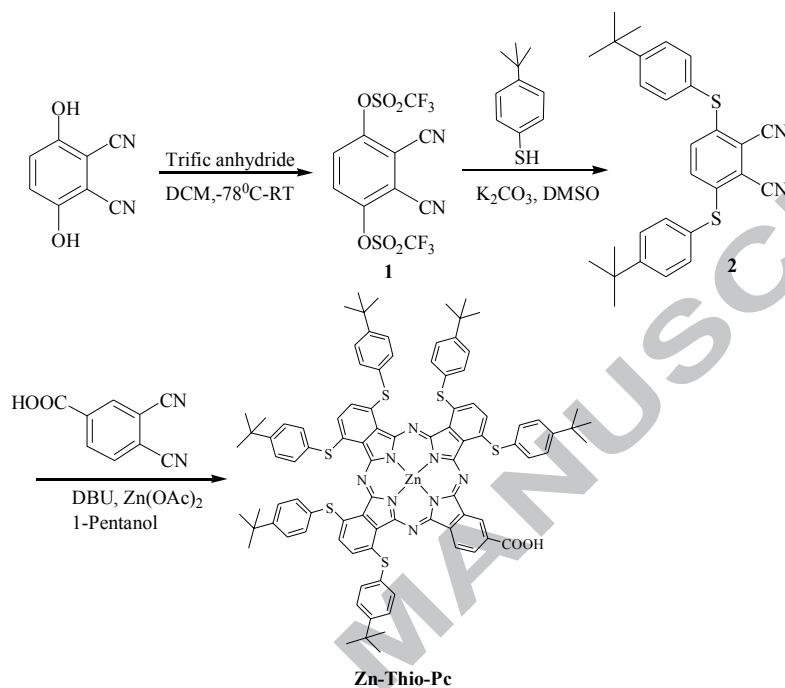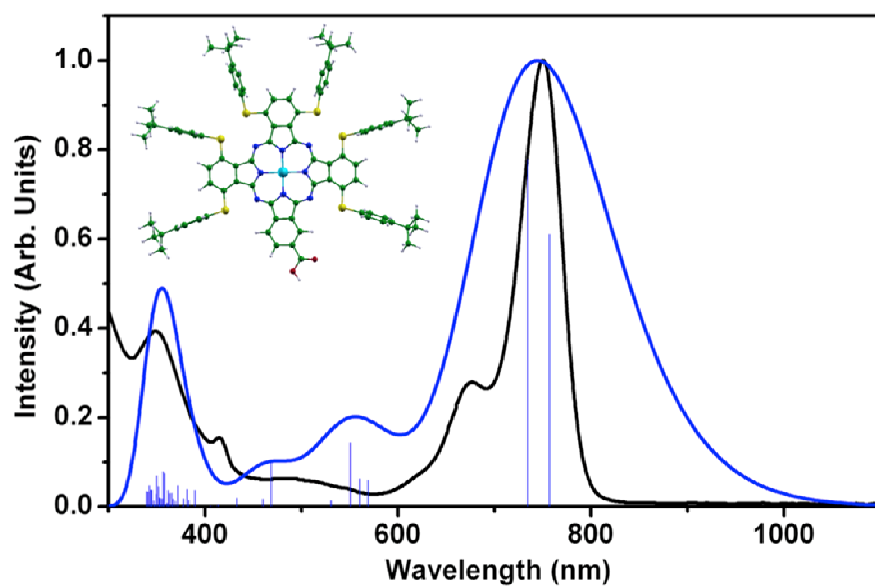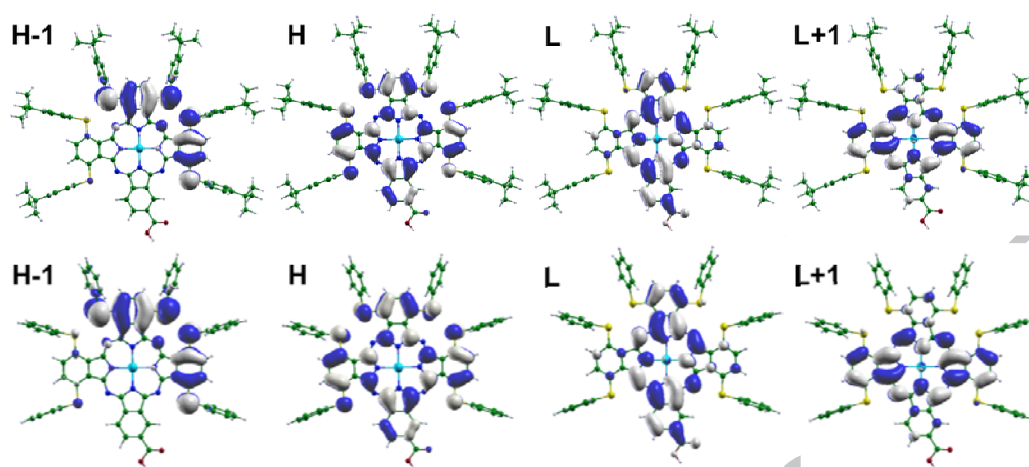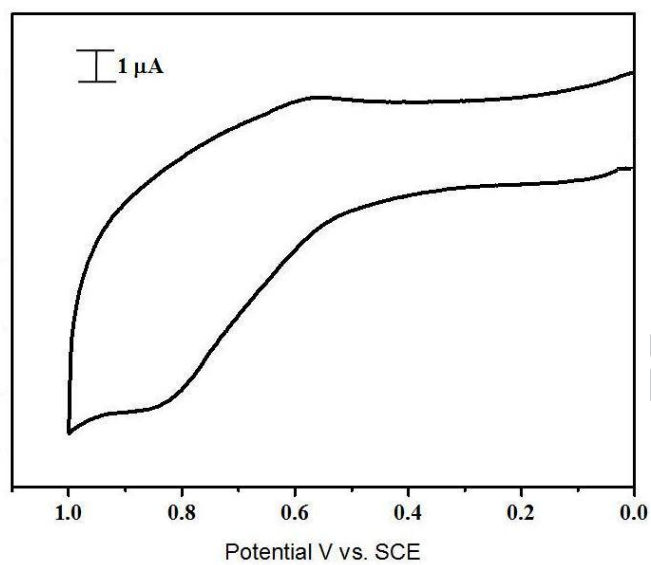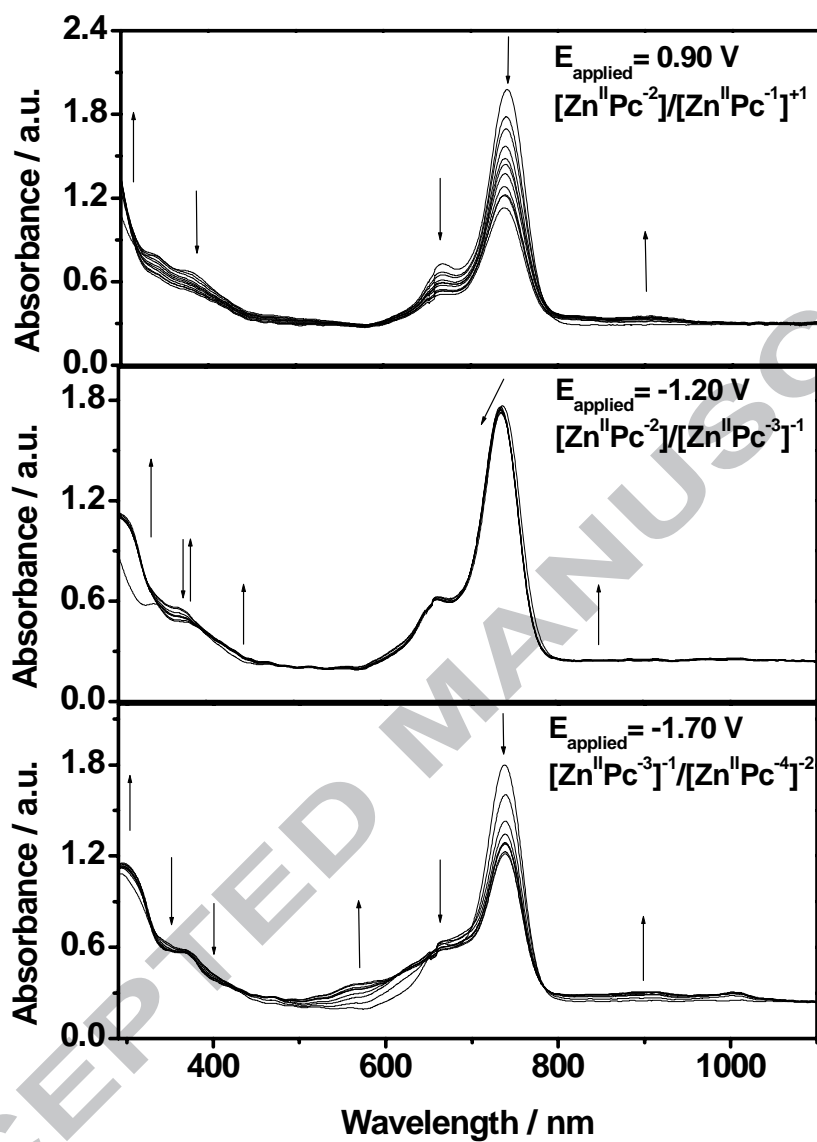
Scheme 1

Fig. 1

Fig. 2

Fig. 3

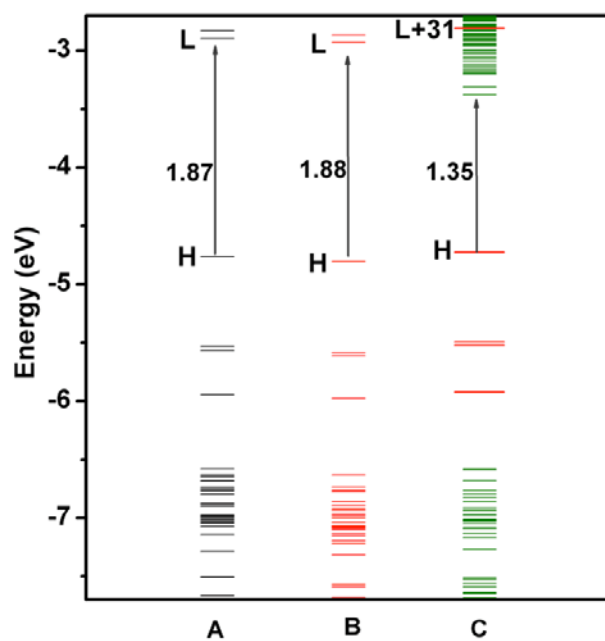Fig. 4
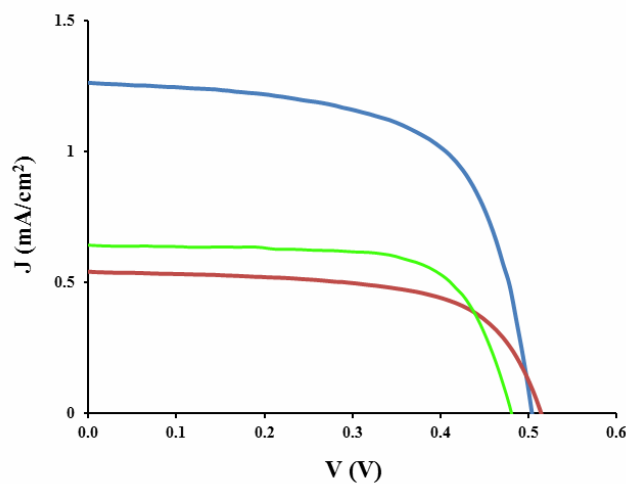
Fig. 5
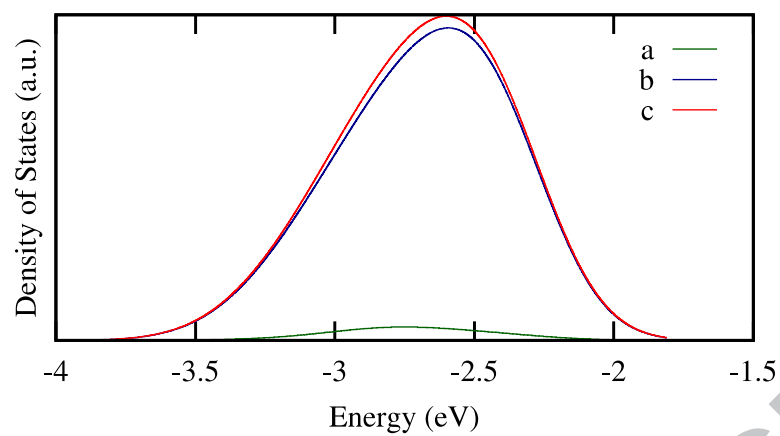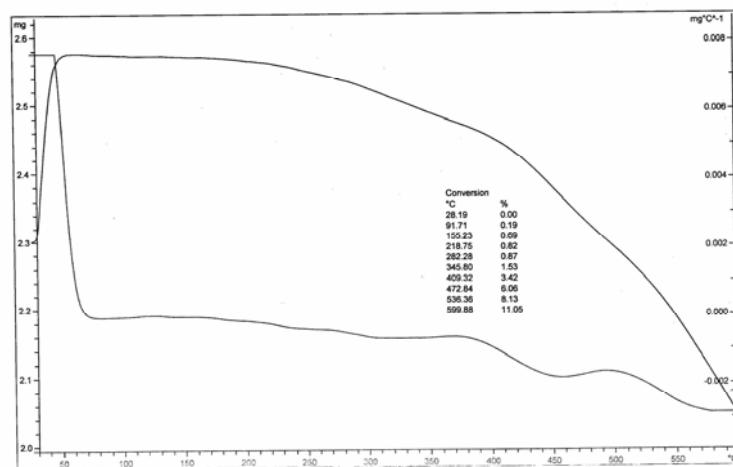
Fig. 6
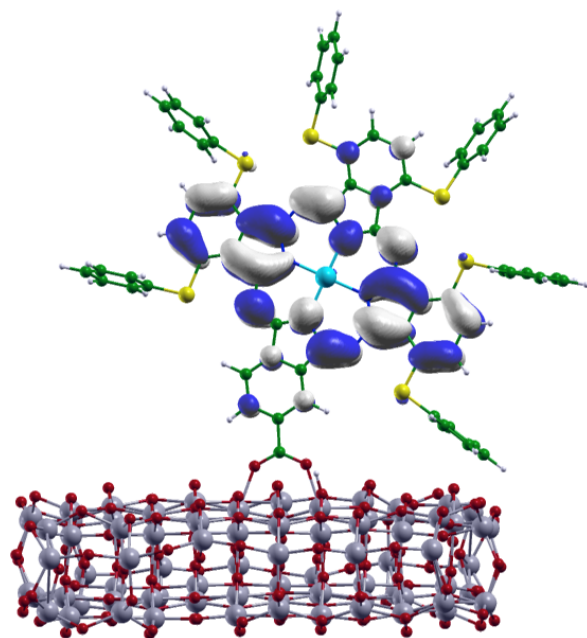
Fig. 7

Fig. 8

Fig. 9

Fig. 10

Table 1. Experimental and calculated wavelengths at major absorption peaks for Zn-Thio-Pc and Zn-Thio-Pc-M systems, along with calculated transitions, oscillator strength (f) in THF solution.

Systems	Exp. (nm/eV)	Calc. (nm/eV)	Trans. (nm/eV)	f	Composition
Zn-Thio-Pc	750/1.65	744/1.67	757/1.64	0.61	H → L (0.70)
			734/1.69	0.78	H → L+1 (0.78)
	677/1.83				
	350/3.54	355/3.49	358/3.46	0.07	H-7 → L+1 (0.33)
			356/3.48	0.08	H-9 → L (0.32)
Zn-Thio-Pc-M		742/1.67	752/1.65	0.59	H → L (0.70)
			731/1.70	0.74	H → L+1 (0.70)
		346/3.58	358/3.46	0.19	H-6 → L (0.33)
			339/3.66	0.17	H-19 → L (0.32)
			338/3.67	0.10	H-2 → L+2 (0.32)

Table 2. Photophysical and electrochemical data of **Zn-Thio-Pc** in THF solvent.

Sample	λ_{max}, nm (log ε, $M^{-1} cm^{-1}$)[a]	λ_{em},[a] nm	(ns) Lifetime	E_{0-0} (eV)[b]	Potential (V, vs. SCE)[c]		E_{ox}^{*d}
					Ox	Red	
Zn-Thio-Pc	350 (4.59) 676 (4.29) 750 (4.84)	778	2	1.66	0.72	-0.98, -1.40	-0.94

[a]Error limits: λ_{max}, ±1 nm, log ε, ±10%. [b]Error limits: ±0.05 eV. [c]Error limits, $E_{1/2}$, ±0.03 V, 0.1 M TBAP. [d]Excited state oxidation potentials are calculated by using $E^* = E_{1/2(OX)}-E_{0-0.}$

Table 3. Photovoltaic parameters for DSCs sensitized with Zn-Thio-Pc dye, measured under simulated AM 1.5G, 1Sun illumination.[a]

Cell	Additives	J_{sc} (mA/cm^2)	V_{oc} (mV)	ff	η (%)
1	No	1.26	502	0.64	0.40
2	CDCA 0.02M	0.54	510	0.51	0.14
3	CDCA 0.005M	0.64	480	0.70	0.22

[a]Photoelectrode: TiO$_2$ (8 + 4 m and 0.158 cm^2); Error limits: Short-circuit photocurrent density, J_{SC}, ±0.1 mAcm^{-2}, Open-circuit voltage, V_{OC}, ±30 mV, Fill factor, ff ±0.03; Electrolyte: 0.6 M 1-butyl-3methylimidiazolium iodide, 0.03 M iodine, 0.1 M LiI, 0.05 M guanidinium thiocyanate, and 0.25 M 4-*tert*-butylpyridine in 15/85 (v/v) mixture of valeronitrile and acetonitrile.

Near-infrared absorbing, unsymmetrical Zn(II) phthalocyanine for dye-sensitized solar cells

V.K Singh, P. Salvatori, A. Amat, S. Agrawal, F. De Angelis, M.K. Nazeeruddin, N.V. Krishna, L. Giribabu
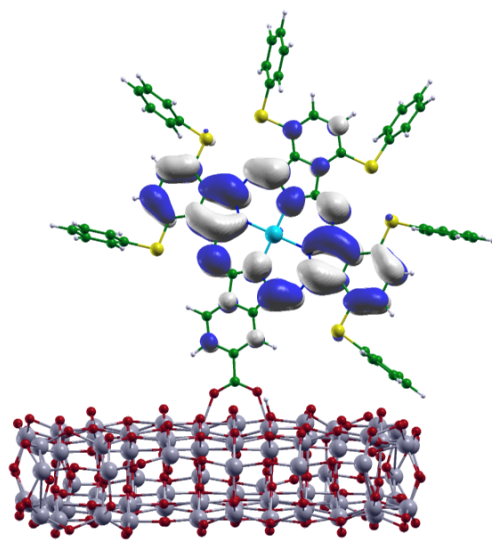
Near-infrared absorbing, unsymmetrical Zn(II) phthalocyanine for dye-sensitized solar cells

V.K Singh, P. Salvatori, A. Amat, S. Agrawal, F. De Angelis, M.K. Nazeeruddin, N.V. Krishna, L. Giribabu

Unsymmetrical Zn(II) phthalocyanine based on 'push-pull' concept. Absorption shifted to N-IR regions. HOMO-LUMO level matched with TiO2 conduction band as well as I⁻/I₃⁻ redox couple.